# EMPLOYING SMARTPHONE AND COMPACT CAMERA IN BUILDING MEASUREMENTS

Haval A. Sadeq

*Salahaddin University-Erbil*
*haval.sadeq@su.edu.krd*

doi:10.23918/iec2018.11

## ABSTRACT

This paper investigates the possibility of implementing images from smartphones and compact cameras for building measurement, such as archaeological buildings, for documentation purposes based on point cloud produced via photogrammetric technique. Images of the object are first captured from different positions. Then, the images are processed for the interior and exterior orientations to produce point cloud. For object registration, one distance is measured at the site, which is assigned to the model and used for scaling. The generated point cloud is subsequently exported into various software, such as AutoCAD, to take measurements or for any architectural studies. Two types of smartphone with different camera resolutions and two types of compact camera are used in the test. Results are validated by comparing several real measurements from the site. The quality of the data is proven to be accurate up to centimetre accuracy.

**Keywords:** smartphone camera, compact camera, point cloud, photogrammetry, archaeological, accuracy.

## 1. INTRODUCTION

Traditional building measurement using tapes is considered to be time consuming, especially at high-altitude areas or areas that have restricted access due to risks, such as ruined archaeological sites. By contrast, using equipment, such as laser scanning, total stations and theodolites, are considered to be expensive because they are time consuming and are designed on specialized people. The task has become difficult because it requires to measure architectural buildings that have complex architectural objects.The evolution of compact digital cameras and smartphone technology, which is accompanied by high-resolution and small size charge-coupled device (CCD) and complementary metal-oxide semiconductor (CMOS), has increased the demand for such equipment. In addition, the decrease in their size and the ease of image capturing have enabled users to carry them in the pocket. This paper focuses on using photogrammetry to generate the model for the building based on point cloud using compact and mobile phone camera. Considering the popularity of photogrammetric software, people can easily process the images for model generation and use it for measurement purposes.Close range photogrammetry is widely used to produce orthomaps for the front view of buildings using metric camera. Subsequently, metric cameras are used to capture image for the purpose of façade reconstruction with the introduction of digital photogrammetry. The development of off-the-shelf and built-in mobile cameras has resulted in the popularity of this system, which is only used for photography. Different studies have been conducted for the purpose of 3D reconstruction, and a method is suggested for interactive 3D model reconstruction based on mobile phones using photogrammetric techniques [1]. Smartphones are used in 3D model generation for the purpose of updating 3D urban maps and detailed enhancements [1]. The accuracy of mobile phone sensors is compared with off-the-shelf cameras, which showed positive results for photogrammetric product implementation [2]. An algorithm least square model image fitting is also [3] implemented by using built-in GPS and image orientation from smartphones as initial values to enhance the exterior image orientation for photogrammetric products that can be used in building construction. [4] assessed the possibility of using mobile phone cameras in UAV for DEM and orthophoto generation. In this study, the images of three buildings are captured using smartphone and compact camera, and point cloud is automatically generated using

CapturingReality software https://www.capturingreality.com/, which is considered for its simplicity. The process is started by loading the captured images in the software, and the photogrammetric process is automatically started to produce point cloud.This paper is structured as follows. Section 1 presents the introduction. Section 2 describes the study area, and Section 3 depicts the implemented camera. Section 4 shows the geometric processing and the result analysis is in Section 5. Finally, Section 6 provides the conclusion.

## 1. STUDY AREA

In this study, three study areas are selected that are located in Erbil-Iraq. The first study area shown in FIGURE 1(a) is referred as study area-1, which is located in Erbil Citadel and represents the rear side of the grand gate at Erbil citadel. This object is considered difficult for surveyors to take measurements at the upper side of the building because it is considered to have high altitude and is difficult to access the top of the building. Study area-2 shown in FIGURE 1(b) is also located in Erbil citadel, which is considered to be an old archaeological building although it has been renovated. The area is displayed for tourists but with limited accessibility, as shown in the figure. A warning tape surrounds this area, and people can only view it because it is considered to be a ruined area. Thus, images are captured at a distance without the users entering the site. These sites are under the supervision of the High Commission for Erbil Citadel Revitalization (HCECR), which is authorized with the control and renovation of the historical building in Citadel. Study area-3 shown in FIGURE 1(c), is considered to be a modern building with different architectural objects and textures. This study area is considered to have smooth surfaces that enable the easy identification of points.


(a) (b) (c)

FIGURE 1. Selected study areas (a) study area-1, citadel gate is considered to be high altitude (b) study area-2 represents the renovated area that has been restricted for users to access (c) study area-3, modern house with different architectural materials and styles.

## 2. IMPLEMENTED SMARTPHONE CAMERA

In this research, four different types of cameras are used for image capture, as shown in FIGURE 2. Two different types of smartphone cameras are used, namely, Samsung smartphone model GT-I9060I with 5 MP and Samsung smartphone J730F Galaxy with 13 MP. In addition, two different compact cameras are used, namely, Canon camera IXUS160 with 20 MP and Sony camera model HX60V with 20.3 MP resolution. These cameras are known as off-the-shelf cameras because they are not specified for photogrammetric purposes and are designed for amateur users.


(a) (b) (c) (d)

FIGURE 2. used mobile phones (a) Samsung smartphone model GT-I9060I resolution 5 MP (b) Samsung smartphone J730F Galaxy 13 MP (c) Canon compact camera IXUS160 resolution 20 MP (d) Sony Compact Camera HX60V resolution 20.4 MP.

As shown in Table 1, two different types of sensors, namely, CCD and CMOS, are adopted in the camera. The two sensors are functioning with similar principle, which is to convert light into electrons, and they are invented at the same period of time. These mobile phones are considered to have small sensor size, which is known

as CMOS. CCD images are considered to have low-noise ratio and less susceptible to noise than CMOS. CMOS sensors are also considered to be less sensitive to light than CCD sensors because they have several transistors located next to them and are considered to consume low battery life, which made them dominant over CCD sensors in mobile phones. Thus, the future of CMOS sensors is the focus of the company [5].

TABLE 1.
Specification of smartphone and compact cameras

| Item | Samsung smartphone model GT-I9060I | Samsung smartphone J730F Galaxy | Canon camera IXUS160 Compact Camera | Sony camera HX60V Compact Camera |
|---|---|---|---|---|
| Sensor resolution | 5 MP | 13 MP | 20 MP | 20.4 MP |
| Sensor type | CMOS | CMOS | CCD | CMOS |
| Image format (pixels) | 2560 x 1920 | 4160 x 3120 | 5152 x 3864 | 5184 x 3888 |
| Focal length (mm) | 2.6 | 3.71 | 5 | 4.3–129 |
| Pixel size(µm) | * | 1.133 | 1.196 | 1.188 |
| Sensor size(mm) | * | 4.73 x 3.49 | 6.16 x 4.62 | 6.16 x 4.62 |
| Crop factor | * | 7.37 | 5.62 | 5.62 |

*Indicates that the information is unavailable.

The number of captured images is varied and is based on the complexity and arrangement of the structure. For instance, the number of captured images in study area-1 is 40 images because the object is façade of building. For study area-2, 96 images are used because the area has different objects, which are considered to be larger than other objects. The captured objects behind the warning tape are shown in FIGURE 1 (b). For study area-3, 60 images are captured because the area is identified to be the façade of the building and has less details than study area-2.

## 3. GEOMETRIC PROCESSING

This stage represents the photogrammetric process, which is achieved in CapturingReality software. At this stage, the images are processed to determine the camera parameters, real position and attitude of images and point cloud generation.

### 3.1. INTERIOR ORIENTATION

Interior orientation is the process that determines the internal geometry of the camera as it used during image capturing, which is designed for calibrated focal length, principal point location, lens the distortion, and sensor size. These parameters are necessary to calculate the actual location of the image space and

remove all the distortions from the image. The parameters of metric camera are obtained at the lab through specific test. For the off-the-shelf camera (used in this paper), two main methods are used for determining the camera parameters, which are known as field test or pre-calibration or through self-calibration [6]. According to the literature, the result of self-calibration can provide more accurate result than pre-calibration [7-10] because it is included in the bundle adjustment process during aerial triangulation. The camera parameter used in this research is based on self-calibration. For the calculation, the initial values are used, such as focal length, image format, ISO speed, and aperture. The initial values of the camera are saved in image metadata known as exchangeable image file format. The cameras used in this study, which are either smartphone or compact camera, are considered to have these parameters. In FIGURE 3, the interior orientation of Samsung SM-J730F is determined, and the lens distortion is plotted on the image, as shown in FIGURE 3(a). The tie point, which is used in parameters determination via self-calibration, is marked. This condition shows that the point is marked on the objects, as shown in FIGURE 3 (b). The parameters of the camera Samsung SM-J730F are shown in FIGURE 3 (c), which are related to focal length, principal point location and lens distortion. The focal length of Samsung SM-J730F is 3.71 mm. However, the value of 27.736067 mm in the determined calibration is based on 35 mm focal length and is equivalent to (35 mm). These equivalent values are selected to compare the viewing angles between different cameras. Camera industries have introduced the term ‘35 mm focal length camera’ [11]. This value can be determined by multiplying the focal length of the camera by focal length multiplier, crop factor or format factor, which is provided by manufacturers (7.37 from TABLE 1). Thus, the calibrated focal length is 3.76 mm.

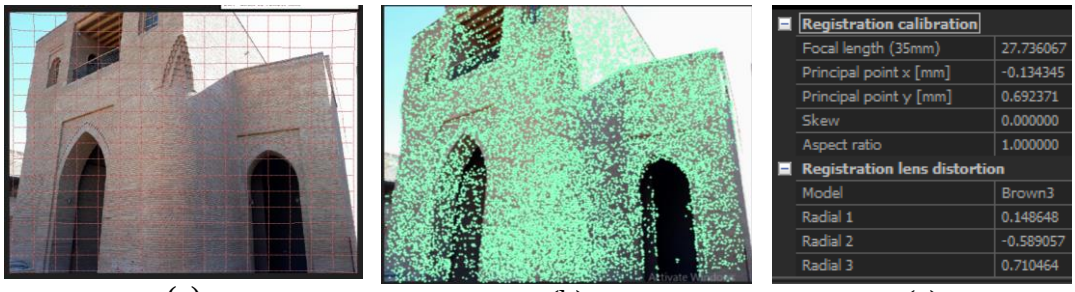


(a) (b) (c)

FIGURE 3. Interior orientation process using camera Samsung SM-J730F for study area-1 (a) shows the amount of distortion that has been affected on the image (b) detected tie point used in calibration (c) screenshot showing the determined parameters of interior orientations.

The model used in this study for the determination of image distortion model is represented in Equation (1), and is used in image correction ascribed by Brown [12]. The model is known as an eight-parameter physical model that is originally developed for film cameras. However, this model is valuable for digital cameras.

$$\begin{aligned} \Delta x &= -x_0 - \frac{\bar{x}}{c}\Delta c + \bar{x}r^2K_1 + \bar{x}r^4K_2 + \bar{x}r^6K_3 + (2\bar{x}^2 + r^2)P_1 + 2P_2\overline{xy} + b_1\bar{x} + b_2\bar{y}; \\ \Delta y &= -y_0 - \frac{\bar{y}}{c}\Delta c + \bar{y}r^2K_1 + \bar{y}r^4K_2 + \bar{y}r^6K_3 + 2P_1\overline{xy} + (2\bar{y}^2 + r^2)P_2; \end{aligned} \quad (1)$$

where $\Delta x$ and $\Delta y$ represent the corrections in x and y directions, respectively; $\bar{x}\ and\ \bar{y}$ are distances from a point to the principal point with respect to x and y directions; $r$ is the radial distance from a point to the principal point; $K_1, K_2\ and\ K_3$ are radial distortion coefficients; $P_1\ and\ P_2$ are coefficients for decentring distortion; and $b_1\ and\ b_2$ represent the affinity of non-orthogonal parameters.

### 3.2. EXTERIOR ORIENTATION

At this stage, the position of images (X, Y and Z) and attitudes ($\omega,\ \varphi,\ k$) are determined. In general, the solution of airborne images for exterior orientation has reached a high precision level, especially with the attached GNSS/IMU information, which subsequently minimized the required GCPs [10, 13, 14]. However, the close-range images are considered challenging, because they rarely have GNSS/IMU instruments attached to the camera due to cost and load issues. Although this condition exists in mobile phones or several cameras, they are considered to have low accuracy, and they can be used as initial values. Thus, different approaches

should be integrated because of the instability of camera calibration process [15, 16]. Although providing data for exterior orientation in close-range photogrammetry is challenging, the images can be processed without providing any information about the image position or orientation. In addition, these approaches can be used to deal with images that are considered to be randomly captured and without sequences. These approaches can process images that have different illuminations and different perceptive views, which are captured from different non-calibrated or non-metric cameras [17-19]. Self-calibration technique is applied to the current photogrammetric tasks, in which the interior orientation is achieved during project implementation or exterior orientation. In this technique, the object points combined with the unknown feature point of interest that appeared in different photos are used in the process [20]. Self-calibration is introduced in Bundle Block adjustment. Thus, camera parameters, such as lens distortion and others, are collectively determined via determination of the object coordinates, which provide more accurate results than test-field calibration [21]. In the photogrammetric process of model registration or absolute orientation (i.e. scaling and georeferencing), seven parameters, namely, three translations, three rotations and one scale parameter [20], are required. This research focuses on distance measurement and does not require the coordinates of the points. Therefore, the model is only adjusted. The distance is measured in the model using tape instrument and is assigned in the model, as shown in FIGURE 4. The same procedure is applied to other study areas.

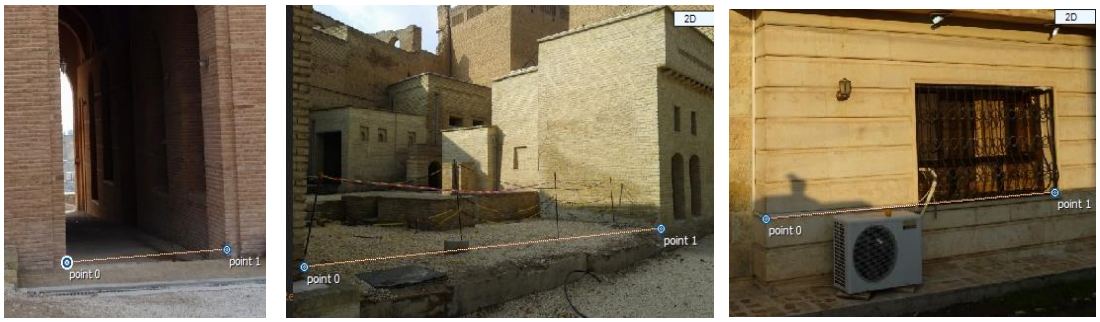


FIGURE 4. Defined distance is shown for the purpose of scaling the models.

### 3.3. POINT CLOUD GENERATION

Apart from image triangulation, images are available for point cloud construction. Point cloud is the result of image matching, which is obtained via collinearity equations. Image matching is considered as the main critical stage in photogrammetry. Different image matching techniques have been developed [22-27]. The technique used in this study is based on the technique that is available in the reality capture software, which is robust for the production of a point cloud, as shown in

FIGURE 5. The technique is not revealed for confidentiality purposes. The common technique that is considered to provide acceptable result is the least square matching, which is based on signal matching that depends on grey values [10]. However, a robust technique, which is called semi-global matching, has been developed. This technique can produce accurate results for 3D object reconstruction. This method requires large overlapping areas [28].

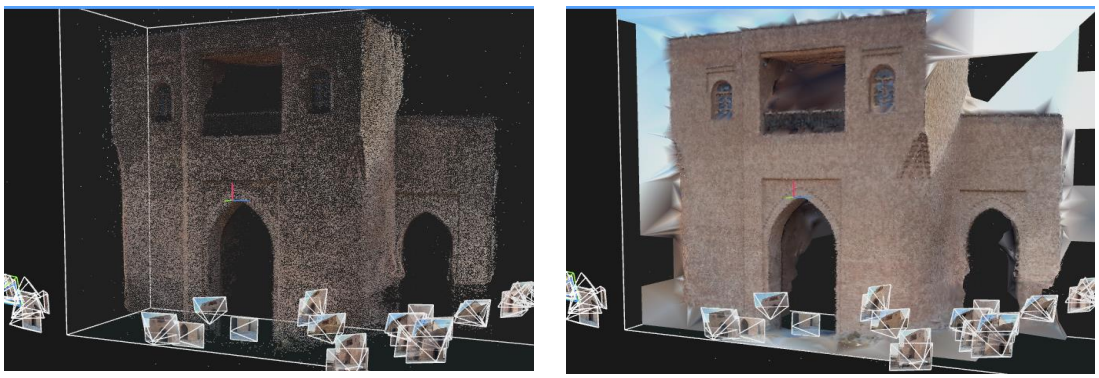

FIGURE 5. Produced point cloud (left image) and rendered object using images from Samsung J7 in study area-1(right image) with camera pose location.

For good visibility, point cloud is rendered for better visualization. The rendering issue is not related to the accuracy of quantity measurement. However, this issue is considered an important requirement for architects to produce realistic views of the object and for good analysis. FIGURE 6 shows the result on study area-2 that has rendered the models from four cameras samples, which shows that all objects are represented. In the rendering model, the roofs of buildings are not generated due to missing photos from the top of the buildings.

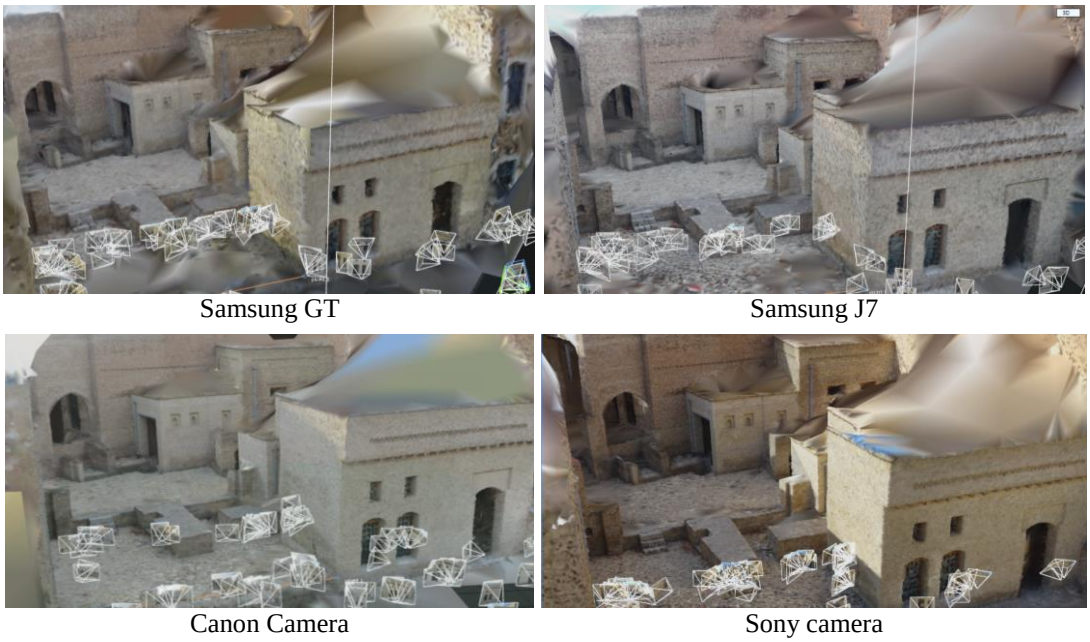


FIGURE 6. Rendered study-area-2, four different rendered models produced from smartphone and compact cameras with the camera pose location.

The produce point cloud model can be used for measurement and documentation purposes to produce a plan view. As shown in FIGURE 7, the top view of study area-2 with all details should produce a map for the site or building layout. The camera did not reach all the areas and has captured images only from one side. However, all the distant walls have been clearly produced.


FIGURE 7. Top view of study area-2 obtained from point cloud, which shows the captured image area and the logo of the ‘reality capturing software’.

## 4. RESULT ANALYSIS

For the model analysis, a set of measurements is selected at three locations. For the assessment, overall 55 different planemetric measurements are used to assess the accuracy of the obtained point cloud. At the site, the distances are obtained from different directions (i.e. in the X, Y and Z directions). Then it is compared with the measurements that are obtained from point cloud using ReCap, as shown in

FIGURE 8. ReCap is built in AutoCAD software, which is designed for laser scanning point cloud measurement. For good point selection of dimensions, the available colour feature in point cloud is clearly represented, which is similar to the point cloud available in laser scanning.

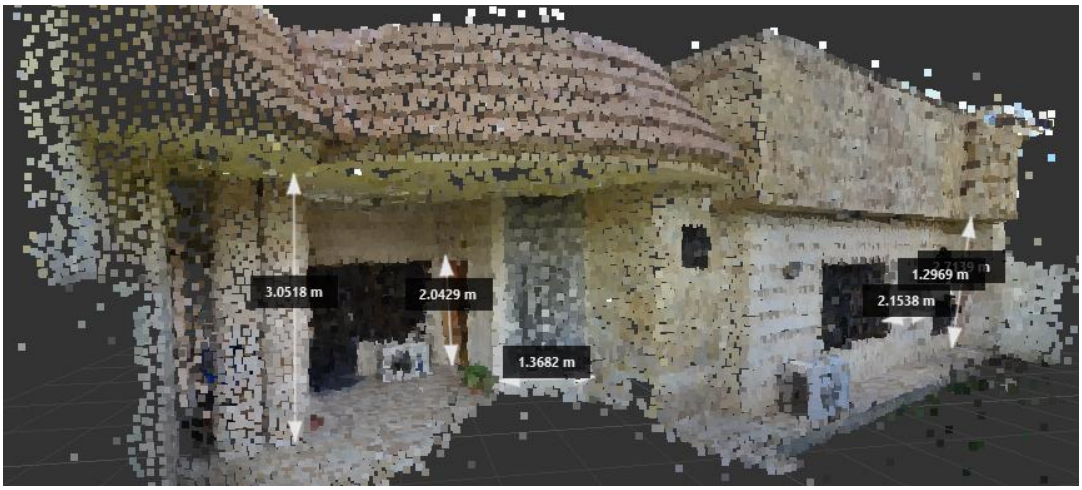


FIGURE 8. Generated point cloud in study area-3 with Sony camera with several measured distances on Autodesk ReCap-2014.

For qualitative analysis, a statistical analysis is applied to the residual. The achieved analysis tests are mentioned in Equations (2), (3) and (4) to obtain the accuracy of the obtained point cloud from each of the mentioned devices in three Study areas, as follows:

$$\mu = \frac{1}{n} \sum_{i=1}^{n} \Delta h_i; \tag{2}$$

$$\sigma = \sqrt{\frac{1}{(n-1)} \sum_{i=1}^{n} (\Delta h_i - \mu)^2}; \tag{3}$$

$$RMSE = \sqrt{\frac{1}{n} \sum_{i=1}^{n} \Delta h_i{}^2}; \tag{4}$$

where $\Delta h_i$ represents the residual or error between the measured distance on point cloud and actual distance, and $\boldsymbol{n}$ represents the number of measurements.

The statistical analysis is listed in TABLE **2**, which shows that the accuracy of point cloud increases with the increase in the resolution of the image. The accuracy in the worst case is less than 0.08 m using smartphone camera. The accuracy is increased to 0.051 in the worst case and 0.35 in the best case with the increase in resolution by using J7. Compact cameras showed better performance than smartphone cameras in terms of study areas 1 and 2, and they are not much different, which is in the worst case less than 0.045 m. For the standard deviations and biases, all the samples for the worst case is 0.61 m and −0.022m, respectively. With the increase in the resolution of sensors, such as Samsung J7 and compact camera, the standard deviation and bias is improved to 0.51 and 0.22 m.

TABLE 2.

Obtained statistical data in analysing the accuracy of point cloud, the accuracy is in in the three directions X,Y, Z.

| | Statistical test | Samsung smartphone model GT-I9060I | Samsung smartphone J730F Galaxy | Canon camera IXUS160 | Sony camera HX60V Compact Camera |
|---|---|---|---|---|---|
| Study area-1 | RMSE (m) | 0.079 | 0.044 | 0.033 | 0.033 |
| | STD (m) | 0.055 | 0.027 | 0.032 | 0.028 |
| | Bias (m) | 0.001 | −0.017 | −0.002 | −0.022 |
| Study area-2 | RMSE (m) | 0.068 | 0.051 | 0.044 | 0.038 |
| | STD (m) | 0.061 | 0.051 | 0.026 | 0.033 |
| | Bias (m) | 0.008 | 0.007 | 0.015 | −0.002 |
| Study area-3 | RMSE (m) | 0.046 | 0.035 | 0.044 | 0.034 |
| | STD (m) | 0.044 | 0.036 | 0.049 | 0.038 |
| | Bias (m) | 0.013 | −0.010 | 0.005 | −0.014 |

## 5. CONCLUSIONS

An efficient technique to obtain the measurements of buildings with reasonable accuracy by using sensors is proposed. This technique is inexpensive and easy-to-use rather than using expensive devices, such as specific photogrammetric cameras. Any type of camera can be used although Samsung mobile phone and Canon Power Shot camera are used in the test. As shown in the result, as the quality of the camera increases the accuracy of the model is increased. The analysis showed that CMOS technology provided better accuracy than CCD under the same resolution. Modern technology has focused on the predominance of CMOS on imaging devices and has obtained more support for improvement from mobile companies.

The technique used in this study can minimize the work needed in documentation. The technique can help obtain quick measurements in the area. In addition, a real 3D model of the object can be obtained and can be used to produce the site layout. The attached colour to the point cloud will help the user identify the points accurately.

## ACKNOWLEDGEMENTS

The author would like to appreciate the CapturingReality company for their cooperation in providing a redeem license to export the data. The author would like to acknowledge HCECR for permitting the access to measure the dimensions of the implemented study area.

## REFERENCES

[1] B. Sirmacek and R. Lindenbergh, "Accuracy assessment of building point clouds automatically generated from iphone images," ISPRS - International Archives of the Photogrammetry, Remote Sensing and Spatial Information Sciences, vol. XL-5, pp. 547-552, 2014.

[2] A. Gruen and M. D. Akca, "Mobile photogrammetry," Vorträge Dreiländertagung SGPBF, DGPF und OVG, vol. 16, pp. 441-451, 2007.

[3] S. Wang, "Toward Automated FAÇADE Texture Generation for 3d Photorealistic City Modelling with Smartphones or Tablet Pcs," ISPRS-International Archives of the Photogrammetry, Remote Sensing and Spatial Information Sciences, pp. 351-354, 2012.

[4] J. Kim, S. Lee, H. Ahn, D. Seo, S. Park, and C. Choi, "Feasibility of employing a smartphone as the payload in a photogrammetric UAV system," ISPRS Journal of Photogrammetry and Remote Sensing, vol. 79, pp. 1-18, 2013.

[5] D. Durini, High performance silicon imaging: fundamentals and applications of cmos and ccd sensors: Elsevier, 2014.

[6] E. Edwards, E. Fey, P. A. Jones, R. K. Jungquist, A. G.LAreau, J. Lebarron, et al., "Cameras and sensing systems," in Manual of Photogrammetry, J. C. McGlone, Ed., ed: American Society for Photogrammetry and Remote Sensing, 2013.

[7] J. S. Aber, I. Marzolff, and J. Ries, Small-format aerial photography: Principles, techniques and geoscience applications: Elsevier, 2010.

[8] S. Harwin, A. Lucieer, and J. Osborn, "The Impact of the Calibration Method on the Accuracy of Point Clouds Derived Using Unmanned Aerial Vehicle Multi-View Stereopsis," Remote Sensing, vol. 7, pp. 11933-11953, 2015.

[9] D. Herrera, C. J. Kannala, and J. Heikkila, "Forget the checkerboard: Practical self-calibration using a planar scene," pp. 1-9, 2016.

[10] T. Rosnell and E. Honkavaara, "Point cloud generation from aerial image data acquired by a quadrocopter type micro unmanned aerial vehicle and a digital still camera," Sensors (Basel), vol. 12, pp. 453-80, 2012.

[11] R. Sheppard, Digital photography: top 100 simplified tips & tricks vol. 25: John Wiley & Sons, 2010.

[12] W. Forstner, B. Wrobel, F. Paderes, C. S. Fraser, J. Dolloff, E. M. Mikhail, et al., "Analytical Photogrammetric Operations," in Manual of Photogrammetry, J. D. McGlone, Ed., Sixth Edition ed Bethesda: American Society of Photogrammetry and Remote Sensing (ASPRS), 2013.

[13] G. Buyuksalih and Z. Li, "Practical experiences with automatic aerial triangulation using different software packages," The Photogrammetric Record, vol. 18, pp. 131-155, 2003.

[14] J. Kremer and E. Kruck, "Integrated Sensor Orientation–Two Examples to show the Potential of simultaneous GPS/IMU and Image Data Processing," Theory, Technology and Realities of Inertial/GPS Sensor Orientation, 2003.

[15] K. Gutjahr, P. Hafner, M. Ofner, K. Längauer, M. Wieser, and N. Kühtreiber, "Performance of GNSS/IMS integration methods in context of a near real-time airborne mapping platform," EuroCOW10, Commission III, WG, vol. 3, 2010.

[16] K.-W. Chiang, H.-W. Chang, C.-Y. Li, and Y.-W. Huang, "An artificial neural network embedded position and orientation determination algorithm for low cost MEMS INS/GPS integrated sensors," Sensors, vol. 9, pp. 2586-2610, 2009.
[17] S. Agarwal, Y. Furukawa, N. Snavely, I. Simon, B. Curless, S. M. Seitz, et al., "Building rome in a day," Communications of the ACM, vol. 54, pp. 105-112, 2011.
[18] M. Brown and D. G. Lowe, "Automatic Panoramic Image Stitching using Invariant Features," International Journal of Computer Vision, vol. 74, pp. 59-73, 2006.
[19] I. Stamos and P. E. Allen, "3-D model construction using range and image data," vol. 1, pp. 531-536, 2000.
[20] K. Kraus, Photogrammetry: geometry from images and laser scans, 2nd ed.: Walter de Gruyter, 2007.
[21] T. A. Clarke and J. G. Fryer, "The development of camera calibration methods and models," The Photogrammetric Record, vol. 16, pp. 51-66, 1998.
[22] N. Haala, "Comeback of digital image matching," in Photogrammetric Week, 2009, pp. 289-301.
[23] W. Tao, Y. Lei, and P. Mooney, "Dense point cloud extraction from UAV captured images in forest area," pp. 389-392, 2011.
[24] F. Leberl, A. Irschara, T. Pock, P. Meixner, M. Gruber, S. Scholz, et al., "Point Clouds," Photogrammetric Engineering & Remote Sensing, vol. 76, pp. 1123-1134, 2010.
[25] A. Gruen, "Development and Status of Image Matching in Photogrammetry," The Photogrammetric Record, vol. 27, pp. 36-57, 2012.
[26] E. Gülch, "Advanced matching techniques for high precision surface and terrain models," in Photogrammetric Week, 2009, pp. 303-315.
[27] M. Pohanka, K. Musilek, and K. Kuca, "Evaluation of aflatoxin B1--acetylcholinesterase dissociation kinetic using the amperometric biosensor technology: prospect for toxicity mechanism," Protein Pept Lett, vol. 17, pp. 340-2, Mar 2010.
[28] H. Hirschmuller, "Stereo processing by semiglobal matching and mutual information," IEEE Trans Pattern Anal Mach Intell, vol. 30, pp. 328-41, Feb 2008.